

Review of predictive capabilities of JRC-JCS model in engineering practice

N. Barton & S. Bandis

Norwegian Geotechnical Institute, Oslo, Norway
& Aristotelian University, Thessaloniki, Greece

ABSTRACT: The database used in developing the Barton-Bandis joint model is reviewed. It is shown how tilt testing to obtain JRC is extrapolated both in terms of stress and sample size. Field measurement of JRC is demonstrated, and relationships with J_r in the Q-system are developed. Constitutive modelling of shear stress-displacement, dilation and shear reversal are also described.

1. INTRODUCTION

The JRC-JCS or Barton-Bandis joint model started inconspicuously some 20 years ago as a means of describing the peak shear strength of more than 200 artificial tension fractures. These were developed with a guillotine in various weak model materials, which had unconfined compression strengths (σ_c) as low as 0.05 MPa.

Linear plots of peak friction angle ($\arctan \tau/\sigma_n$) versus peak dilation angle (d_n) indicated the following simple expression:

$$\tau = \sigma_n \tan(2d_n + 30^\circ) \quad (1)$$

It was found that the peak dilation angle was proportional to the logarithm of the ratio (σ_c/σ_n):

$$d_n = 10 \log(\sigma_c/\sigma_n) \quad (2)$$

By elimination, the following simple form was obtained

$$\tau = \sigma_n \tan[20 \log(\sigma_c/\sigma_n) + 30^\circ] \quad (3)$$

Thus the first form of the "JRC-JCS" model was actually the "20 - σ_c " model, where the roughness coefficient (JRC) was equal to 20 for these rough tension fractures. The joint wall strength (JCS) was equal to σ_c (the unconfined compression strength). The original form of the equation is therefore perfectly consistent with today's equation:

$$\tau = \sigma_n \tan[JRC \log(JCS/\sigma_n) + \phi_r] \quad (4)$$

and represents the three limiting values of the three input parameters i.e.

$$JRC = 20 \text{ (roughest possible joint without actual steps)}$$

$$JCS = \sigma_c \text{ (least possible weathering grade, i.e. fresh fracture)}$$

$$\phi_r = \phi_b \text{ (fresh unweathered fracture with basic friction angles in the range } 28\frac{1}{2} \text{ to } 31\frac{1}{2}^\circ \text{)}$$

In addition, the small size of the samples (60 mm length) meant that both JRC and JCS were truly laboratory scale parameters and would nowadays be given the subscripts JRC_0 and JCS_0 (Barton et al. (1985), to distinguish them from the scale-corrected full scale values JRC_n and JCS_n (see later).

2 PEAK STRENGTH OF ROCK JOINTS AND ITS PREDICTION

Figure 1 illustrates the results of direct shear tests, on 130 rock joints, reported by Barton and Choubey (1977). Eight rock types were represented. The statistics for JRC, JCS and ϕ_r are given in Figure 2. The mean values of these parameters

$$JRC = 8.9 \quad JCS = 92 \text{ MPa} \quad \phi_r = 28^\circ$$

were used as input parameters to derive the central strength envelope in Figure 1.

A key aspect of this study was the discovery that self-weight tilt testing,

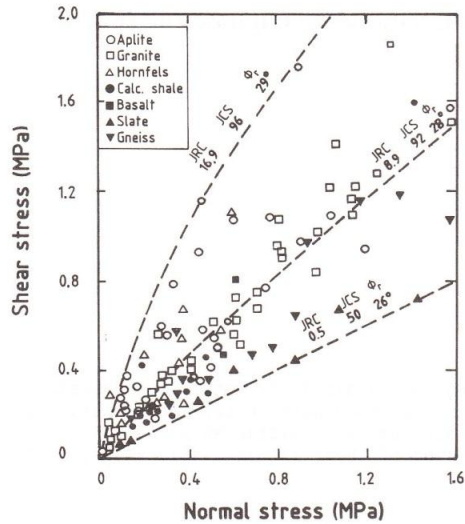


Fig. 1. Peak shear strength of 130 rock joints and strength prediction with equation 4.

such as that illustrated in Figure 3, could be used to predict peak shear strength. Based on tilt tests of the 57 joint samples with $JRC \leq 8.0$, a mean value of peak friction angle ($\phi = \arctan \tau/\sigma_n$) of 40.3° was predicted for the 57 direct shear tests that followed the tilt testing. The measured mean was 40.5° , a 0.2° error.

The tilt tested joint sample generally reaches failure when the normal stress is as low as 0.001 MPa. Remarkably, equation 4 gives a reasonably accurate estimate of peak friction angle up to normal stress levels approaching five orders of magnitude higher.

At stress levels approaching the level of σ_c (or JCS), substitution of the confined strength ($\sigma_1 - \sigma_3$) in equation 4 in place of σ_c (or JCS) gives a very good fit to the shear strength of fresh fractures. Asperities apparently develop higher strength due to their increased confinement with the greater areas of contact (Barton, 1976):

$$\tau = \sigma_n \tan \left[JRC \log \left(\frac{\sigma_1 - \sigma_3}{\sigma_n} \right) + \phi_r \right] \quad (5)$$

The logarithmic form of equations 4 and 5 means that the peak friction angle increases by JRC degrees for every order of magnitude reduction in normal stress.

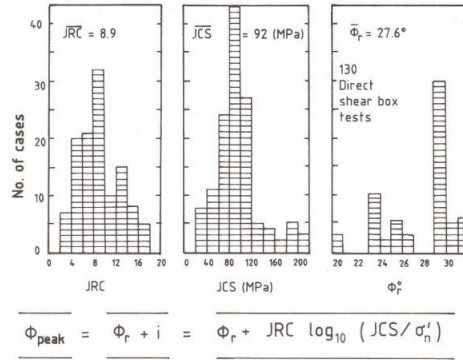


Fig. 2. JRC, JCS and ϕ_r statistics for 130 joints.

Table 1 illustrates this with example values of $JRC = 5$ and 10 , and $JCS = 100$ MPa. Typical tilt angles (α°) at failure would be expected to be about 55° and 80° respectively. Since tilt angles approaching 90° present experimental difficulties (toppling before sliding) and theoretical difficulties (cohesion intercept), the use of tilt tests for joints with JRC values greater than about 10 is generally impossible and horizontal pull tests must be used. The general formula for evaluating tilt tests is:

$$JRC = \frac{\alpha - \phi_r}{\log \left[\frac{JCS}{\sigma_n} \right]} \quad (6)$$

3 DILATION OF ROCK JOINTS AND ITS PREDICTION

Asperity angles (i) of about 60° will be sufficient to give true cohesion intercepts and prevent tilt testing. In effect the joint experiences a peak dilation angle of equal magnitude to the (i) value.

Peak dilation angles recorded in the direct shear tests shown in Figure 1 varied from 0° to 60° with an average value of 20.0° . At low normal stress levels, with little asperity damage, the peak dilation angle can be approximated by:

$$d_n = JRC \log(JCS/\sigma_n) \quad (7)$$

At higher normal stress, with increasing asperity damage the peak dilation angle may reduce to as low as:

Table 1 Effect of large stress changes on peak friction angles for example values of JRC = 5 or 10, JCS = 100 MPa and $\phi_r = 30^\circ$.

arctan (τ/σ_n)	σ_n (MPa)	arctan (τ/σ_n)°		σ_n (MPa)	Comments
		JRC=5	JRC=10		
$>\phi_r$	JCS·1	$>30^\circ$	$>30^\circ$	100	JCS = $\sigma_1 - \sigma_3$ $i = \text{JRC}$
$\phi_r + \text{JRC}$	JCS·10 ⁻¹	35°	40°	10	
$\phi_r + 2 \text{ JRC}$	JCS·10 ⁻²	40°	50°	1	
$\phi_r + 3 \text{ JRC}$	JCS·10 ⁻³	45°	60°	0.1	
$\phi_r + 4 \text{ JRC}$	JCS·10 ⁻⁴	50°	70°	0.01	
$\phi_r + 5 \text{ JRC}$	JCS·10 ⁻⁵	55°	80°	0.001	

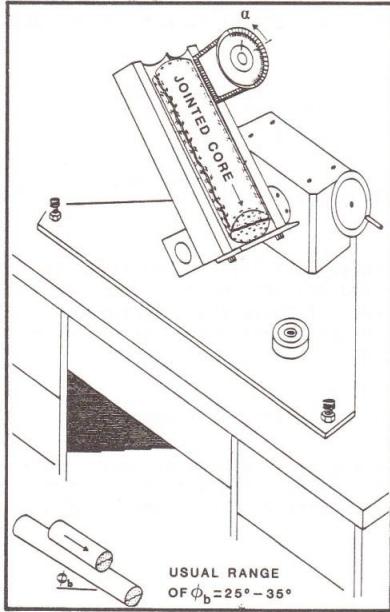
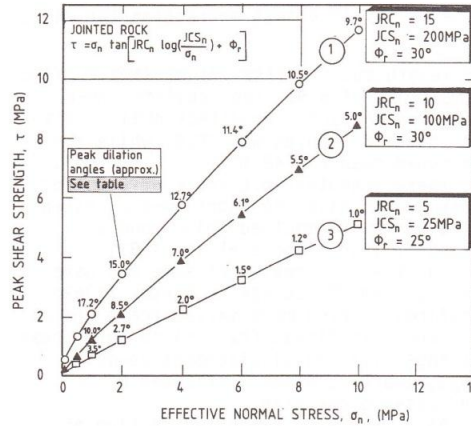


Fig. 3. Tilt test for JRC and ϕ_b .

$$d_n = \frac{1}{2} \text{JRC} \log(\text{JCS}/\sigma_n) \quad (8)$$

To illustrate the importance of dilation angles to the behaviour of rock joints in confined situations, the strength envelopes drawn in Figure 4 have been appended the minimum likely values of d_n (from equation 8). It is likely that the dilation angles are even higher for envelope 1 thereby emphasising the great importance of both joint roughness and joint wall strength in the stability of underground openings.



Estimates of peak dilation angles (d_n)

Curve no.	Effective normal stress (MPa)							
	0.1	0.5	1.0	2.0	4.0	6.0	8.0	10.0
1	24.7	19.5	17.2	15.0	12.7	11.4	10.5	9.7
2	15.0	11.5	10.0	8.5	7.0	6.1	5.5	5.0
3	6.0	4.2	3.5	2.7	2.0	1.5	1.2	1.0

Fig. 4. Peak dilation angles appended to shear strength envelopes (Barton, 1987).

4 SCALE EFFECT AND ITS PREDICTION

Pratt et al. (1974) indicated in their tests on joints in quartz diorite that peak friction angles reduced from 68° to 48° when sample length was increased from 14 to 71 cm. A common normal stress of 1.5 MPa was employed. According to theoretical calculations by Barton and Choubey (1977) utilizing equation 4, some 12° to 15° of this scale effect may have been caused by reduced JCS, the remainder by scale effects on JRC. The last authors reported JRC values of 5.5 for tilt tests of a 45 cm long joint in granite. Tilt and push tests on 18 small samples of 10

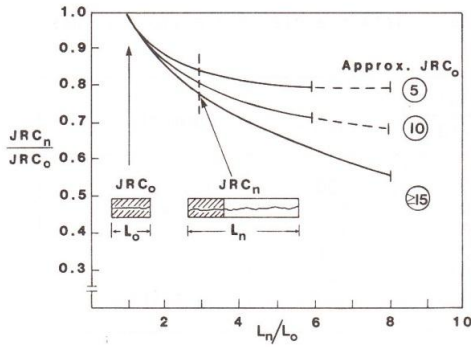


Fig. 5a. Scale effect correction for JRC_0 .

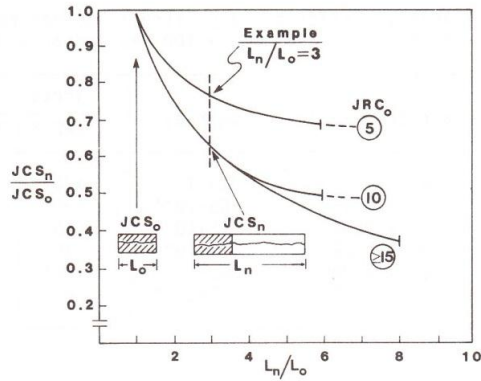


Fig. 5b. Scale effect correction for JCS_0 .

cm length cut from the larger sample, gave a mean JRC of 8.8. The predicted mean value of $\phi(\text{peak})$ from direct shear tests on these 18 samples was 48.8, while the measured mean was 48.5°.

These incontestable scale effects for rock joints have been confirmed by extensive work with moulded joint models. (Bandis, 1980, Bandis et al. 1981).

An extensive review of some 650 data points from 35 sources by Barton (1982) confirms an even more marked scale effect for shear stiffness (K_s), since both shear strength (τ) and displacement-to-peak (δ_{peak}) are separately affected by increased block size.

As a result of extensive testing of joints, joint replicas, and review of literature, Barton and Bandis (1982) proposed scale correction curves for JRC and JCS as shown in Figure 5 and in equations 9 and 10.

$$JRC_n \approx JRC_0 \left[\frac{L_n}{L_0} \right]^{-0.02 JRC_0} \quad (9)$$

$$JCS_n \approx JCS_0 \left[\frac{L_n}{L_0} \right]^{-0.03 JRC_0} \quad (10)$$

where subscripts (o) and (n) refer to lab scale (100 mm) and in situ block sizes. The effect of these scale factors on stress-displacement curves is shown in Figure 6.

5 FIELD ESTIMATION OF ROUGHNESS

A quick way of obtaining an approximate measure of JRC_n using a straight edge is shown in Figure 7. The roughness of a

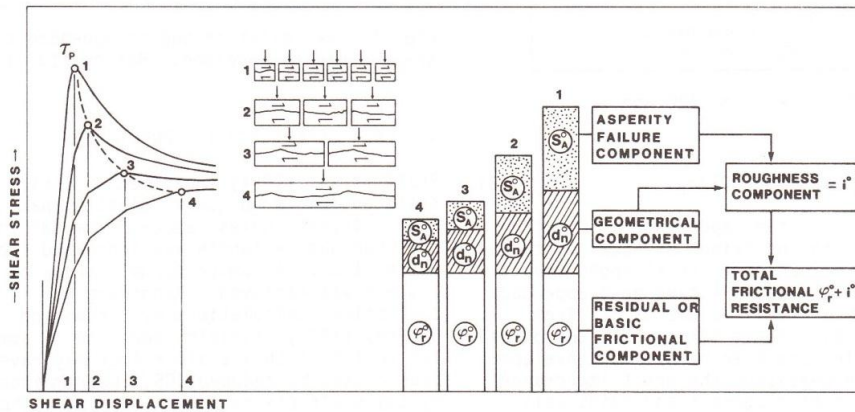


Fig. 6. Components of shear strength and their reduction with increased block size indicates the complexity of Patton's "i" value in practice, Bandis (1980).

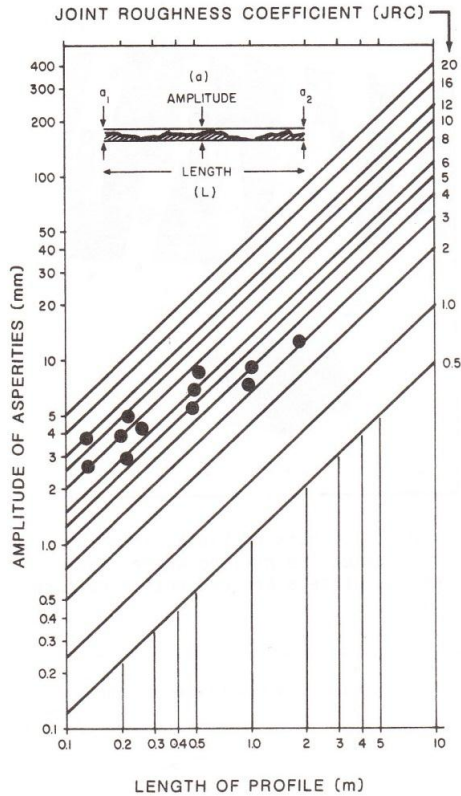


Fig. 7. Field estimate of JRC_n prior to tilt testing (Barton 1982).

joint in the field can also be described by the parameter J_r , borrowed from the Q-system (Barton et al. 1974). Suggested values are summarized in Table 2 and Figure 8. The field method of estimating JRC_n shown in Figure 7 has been used directly to suggest JRC_n values for 20 cm and 100 cm sized blocks (Figure 8, right-hand columns). Combined use of J_r and J_a

Table 2. The Q-system parameter J_r .

3. JOINT ROUGHNESS NUMBER	
(a) Rock wall contact and (b) Rock wall contact before 10 cms shear	(J_r)
A. Discontinuous joints	4
B. Rough or irregular, undulating	3
C. Smooth, undulating	2
D. Slickensided, undulating	1.5
E. Rough or irregular, planar	1.5
F. Smooth, planar	1.0
G. Slickensided, planar	0.5

Note: (i) Descriptions refer to small scale features and intermediate scale features, in that order.

Relation between J_r and JRC_n Subscripts refer to block size (cm)		J_r	JRC_{20}	JRC_{100}
I	rough	4	20	11
	smooth			
	slickensided			
Stepped				
IV	rough	3	14	9
	smooth			
	slickensided			
Undulating				
VII	rough	1.5	7	6
	smooth			
	slickensided			
Planar				
VII	rough	1.5	2.5	2.3
	smooth			
	slickensided			
IX	rough	1.0	1.5	0.9
	smooth			
	slickensided			
IX	rough	0.5	0.5	0.4
	smooth			
	slickensided			

Fig. 8. Relationships between J_r in the Q-system and JRC_n for 200 mm and 1000 mm samples (Barton, 1987).

(Table 3) from the Q-system also provides a means of obtaining a first estimate of peak friction angles for unweathered and mineral coated joint walls using the simple relation in Table 4.

Field estimation of input parameters for the two simple constitutive models illustrated in Figure 9, can be supplemented with tilt tests on extracted blocks containing the joint in question (Figure 10). Alternatively, joints in drill core can be tilt tested, using standard drill core or using dedicated large diameter cores drilled parallel with joint planes.

Table 3. The Q-system parameter J_a .

4. JOINT ALTERATION NUMBER	(J_a)	(ϕ_p) (approx.)
(a) Rock wall contact		
A. Tightly healed, hard, non-softening, impermeable filling i.e. quartz or epidote	0.75	(-)
B. Unaltered joint walls, surface staining only	1.0	(25-35°)
C. Slightly altered joint walls. Non-softening mineral coatings, sandy particles, clay-free disintegrated rock etc.	2.0	(25-30°)
D. Silty-, or sandy-clay coatings, small clay fraction (non-soft.)	3.0	(20-25°)
E. Softening or low friction clay mineral coatings, i.e. kaolinite or mica. Also chlorite, talc, gypsum, graphite etc., and small quantities of swelling clays.	4.0	(8-16°)

Figure 11 illustrates three axially jointed cores with the actual measured roughness profiles placed at the measured tilt angles (69.8° to 72.1°). JRC values calculated using equation 6 ranged from 7.9 to 8.3.

6 SHEAR STRESS - DISPLACEMENT AND ITS PREDICTION

A dimensionless formulation for estimating the correct shape of shear stress displacement curves for any practical normal

Table 4. Estimate of ϕ (peak) from J_r and J_a .

(a) Rock wall contact	J_r	$\tan^{-1} (J_r/J_a)^{0.5}$				
		$J_a=0.75$	1.0	2	3	4
A. Discontinuous joints	4	79°	76°	63°	53°	45°
B. Rough, undulating	3	76°	72°	56°	45°	37°
C. Smooth, undulating	2	69°	63°	45°	34°	27°
D. Slickensided, undulating	1.5	63°	56°	37°	27°	21°
E. Rough, planar	1.0	53°	45°	27°	18°	14°
F. Smooth, planar	0.5	34°	27°	14°	9.5°	7.1°

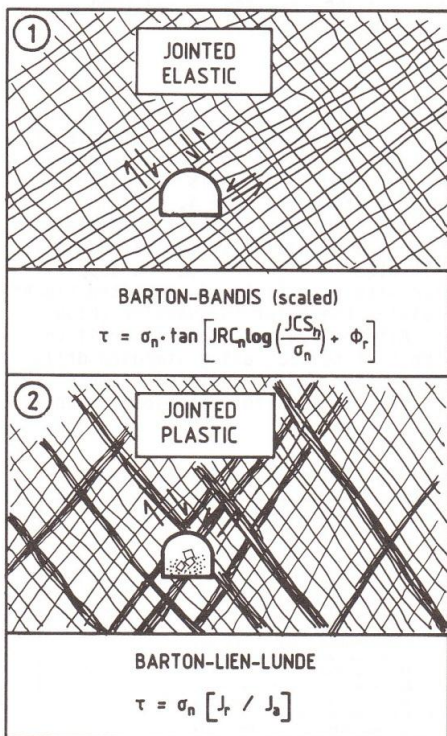


Fig. 9. Shear strength criteria for rock masses.

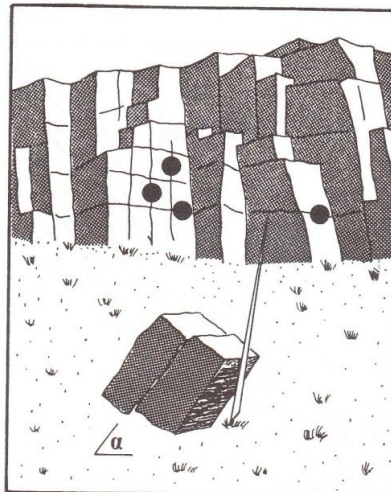


Fig. 10. Tilt tests of blocks in situ. Large cores can be drilled where insufficient joint sets are present to release blocks.

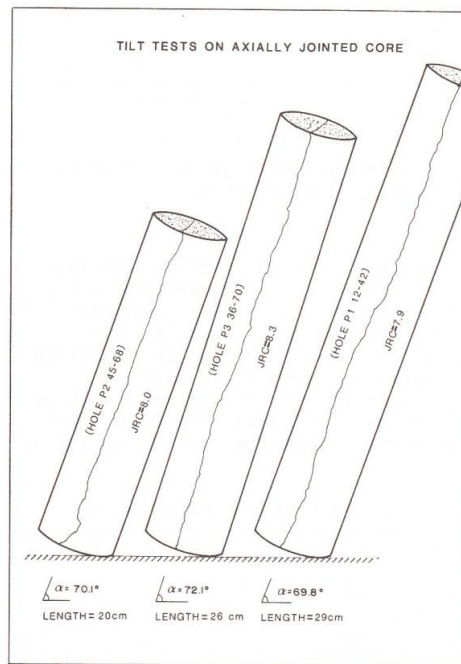


Fig. 11. Reconstructed tilt test results for three parallel core samples drilled down the same joint plane.

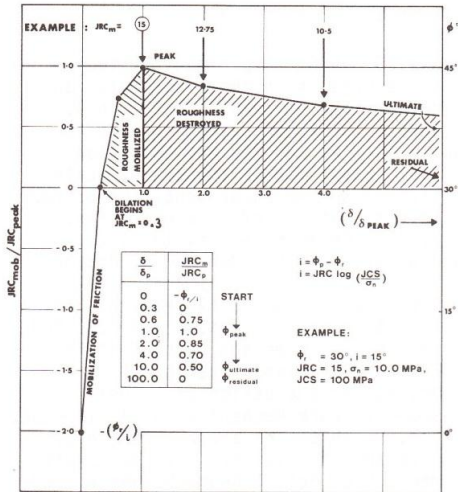


Fig. 12. Dimensionless model for shear stress-displacement modelling, after Barton (1982). In this example $\phi_r/i = 2$.

stress level or block size, is illustrated in Figure 12. Three examples are shown in Figure 13.

The value of JRC (mobilized) is obtained from the generalized form of equation 4; where $\phi(\text{mob})$ is the friction angle mobilized at any given shear displacement (δ):

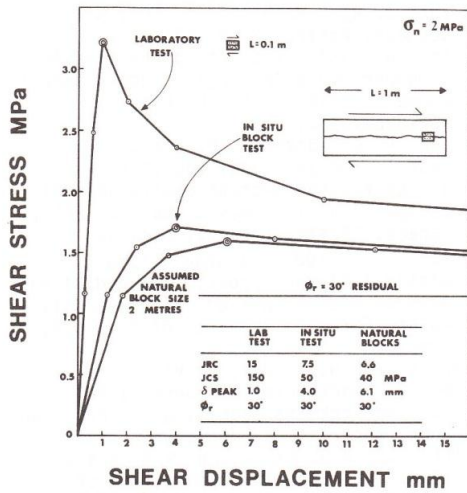


Fig. 13. Examples of stress-displacement curves calculated from the model in Figure 12.

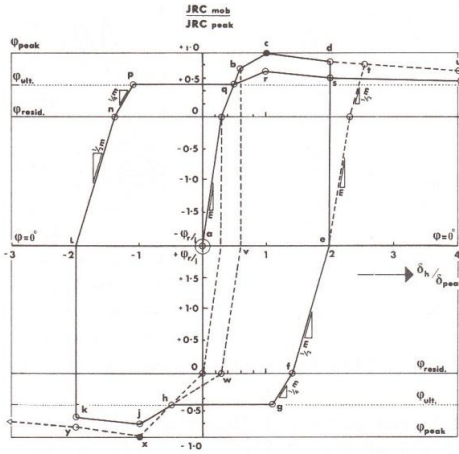


Fig. 14. A preliminary model for simulating the effects of cyclic shear and accumulated shear for rock joints.

$$\phi_{\text{mob}} = JRC_{\text{mob}} \log \left[\frac{JCS_{\eta}}{\sigma_n} \right] + \phi_r \quad (11)$$

The magnitude of $\delta(\text{peak})$ representing the displacement needed to mobilize peak shear strength, is approximated by the equation:

$$\delta_{\text{peak}} = \frac{L_n}{500} \left[\frac{JRC_n}{L_n} \right]^{0.33} \quad (12)$$

where $\delta(\text{peak})$ and L_n are in meters. This equation was a somewhat poor "best fit" to 650 test data points obtained by the authors and gleaned from the literature.

Shear reversal, with or without change of normal stress, can be approximated with the dimensionless formulation shown in Figure 14, where (m) is the initial gradient in Figure 12:

$$m = \frac{\phi_r}{i(0.3)} \quad (13)$$

7 NUMERICAL MODELLING OF JOINTED ROCKMASSES

The above formulations (equations 4, 8, 9, 10, 11, 12, 13 and Figures 12 and 14) are incorporated in the special version of Cundall's UDEC code (Cundall, 1980), operated by NGI. The non-linear, scale dependent joint model described in the above is also developed for normal closure and aperture modelling (Bandis et al).

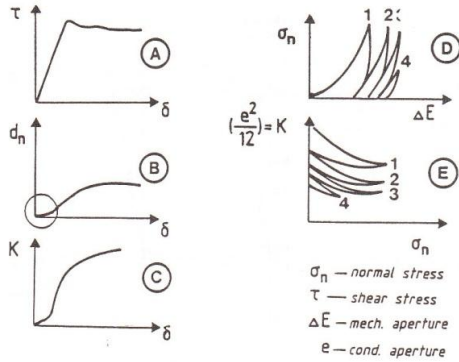


Fig. 15. Five basic joint behaviour modes.

1983) and for fluid flow along the joints (Barton et al. 1985). The operating code, termed UDEC-BB, has a subroutine for joint behaviour that includes the features shown in Figure 15: A = shear stress-displacement, B = dilation-displacement, C = permeability-displacement, D = normal stress-closure (multiple cycles) and E = permeability-normal stress. Modelled rock masses display combinations of these modes (see Figure 16). The UDEC-BB model of twin tunnels shown in Figure 17, shows the stabilizing effect of shear displacement and dilation which causes increased normal stress (Makurat et al. 1990).

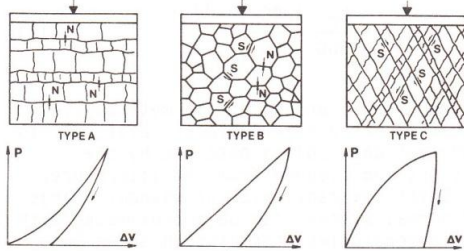


Fig. 16. Normal (N) and shear (S) components in rock mass deformation behaviour

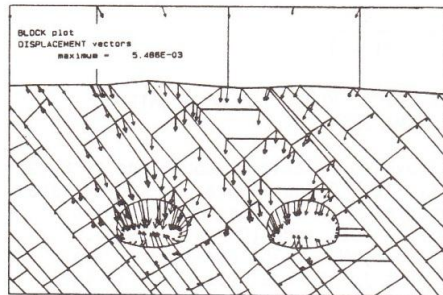


Fig. 17. Max. displacement 5.5 mm; UDEC-BB

REFERENCES

- Bandis, S. 1980. Experimental studies of scale effects on shear strength, and deformation of rock joints. Ph.D. Thesis, Univ. of Leeds, England, 385.
- Bandis, S., A. Lumsden and N. Barton 1981. Experimental studies of scale effects on the shear behaviour of rock joints, *Int. J. of Rock Mech. Min. Sci. & Geomech. Abstr.* 18, 1-21.
- Bandis, S., A.C. Lumsden and N. Barton 1983. Fundamentals of Rock Joint Deformation. *Int. J. Rock Mech. Min. Sci. & Geomech. Abstr.* 20, 6, 249-268.
- Barton, N., R. Lien and J. Lunde 1974. Engineering classification of rock-masses for the design of tunnel support, *Rock Mechanics*, 6, 4, 189-236.
- Barton, N. 1976. The shear strength of rock and rock joints, *Int. Jour. Rock Mech. Min. Sci. & Geomech. Abstr.*, 13, 9, 255-279. Also NGI-Publ. 119, 1978.
- Barton, N. and V. Choubey 1977. The shear strength of rock joints in theory and practice, *Rock Mechanics*, 1/2, 1-54. Also NGI-Publ. 119, 1978.
- Barton, N. 1982. Modelling rock joint behavior from in situ block tests: Implications for nuclear waste repository design, ONWI-308, Columbus, OH, 96
- Barton, N. and Bandis, S. 1982. Effects of Block Size on the Shear Behavior of Jointed Rock, 23rd U.S. Symp. on Rock Mech., Berkeley, CA. 739-760.
- Barton, N., Bandis, S. and Bakhtar, K. 1985. Strength, Deformation and Conductivity Coupling of Rock Joints, *Int. J. Rock Mech. & Min. Sci. & Geomech. Abstr.* 22, 3, 121-140.
- Barton, N. 1987. Predicting the Behaviour of Underground Openings in Rock. Manuel Rocha Memorial Lect., Lisbon. NGI-Publ. 172.
- Barton, N. and Bakhtar, K. 1987. Description and modelling of rock joints for the hydrothermalmechanical design of nuclear waste vaults. AECL, Canada, TR-418, I and II, 1-429.
- Cundall, P.A. 1980. A Generalized Distinct Element Program for Modelling Jointed Rock PCAR-1-80. Peter Cundall Assoc. European Research Office, U.S. Army.
- Makurat, A., N. Barton, G. Vik, P. Chryssanthakis, K. Monsen 1990. Jointed Rockmass modelling. Proc. Loen Conf. Rock Joints, Norway.
- Pratt, H.R. A.D. Black, and W.F. Brace 1974. Friction and Deformation of Jointed Quartz Diorite, Proc. of 3rd Int. Cong. on Rock Mech., Denver, CO, 2A, 306-310.